Limnol. Oceanogr., 49(5), 2004, 1742–1753

Relationships among photoperiod, carbon fixation, growth, chlorophyll *a*, and cellular iron and zinc in a coastal diatom

William G. Sunda and Susan A. Huntsman
National Ocean Service, National Oceanic and Atmospheric Association, 101 Pivers Island Road, Beaufort, NC 28516

Abstract

We conducted culture experiments with the diatom *Thalassiosira pseudonana* to determine the interactive effects of day length and biologically available concentrations of iron and zinc on cellular iron (Fe), zinc (Zn), chlorophyll *a* (Chl *a*), and fixed carbon (C) throughout the light period. Specific rates of C-fixation and growth were also measured. Specific C-fixation rates showed a single linear relation with the cellular Fe : C ratio regardless of the photoperiod. Decreasing the photoperiod from 14 to 7 h increased the mean daytime cellular Fe : C ratio by 40%, the specific C-fixation rate by 34%, and the Chl *a* : C ratio by 91% in mildly iron-limited cultures. These changes reflect a cellular acclimation to the shortened light period. The higher cellular iron level apparently allowed for synthesis of additional iron-rich proteins (e.g., those utilized in photosynthetic electron transport) needed to support the increased rate of C-fixation. Mean cellular Chl *a* concentration decreased linearly with decreasing specific growth rate under iron and zinc limitation, thereby allowing the cells to maintain a balance between light harvesting and biosynthesis. Cellular concentrations of carbon, Chl *a*, zinc, and iron typically varied during the light period because of the day–night differences in rates of C-fixation, Chl *a* synthesis, growth, and metal uptake. Cell carbon concentrations increased by 36–96% during the light period, reflecting daytime storage of fixed carbon to support nighttime respiration and growth. Cellular zinc concentrations decreased by 25% during the light period owing to higher daytime specific growth rates and resulting higher rates of biodilution. By contrast, the direction of change in cellular iron concentrations was dependent on the extent of photochemical redox cycling of iron chelates, which increased iron uptake rates during the day. The direction and magnitude of daytime changes in cellular zinc and iron were also dependent on the parameter (cell volume, cell numbers, or carbon) to which the cellular metal was normalized, as each of these parameters exhibited its own unique diurnal pattern.

Micronutrient metals (iron, zinc, and cobalt) play a significant role in regulating the growth and species composition of marine phytoplankton (Morel and Price 2003). Iron (Fe) regulates phytoplankton growth and food web structure in major regions of the ocean, including the subarctic and equatorial Pacific (Martin and Fitzwater 1988; Coale et al. 1996), the Southern Ocean (Boyd et al. 2000), and some coastal upwelling systems (Hutchins et al. 1998). Zinc (Zn) is less important in limiting marine productivity (Coale 1991) but, in conjunction with cobalt (Co), may affect phytoplankton community structure through differences in growth requirements among algal species (Brand et al. 1983; Sunda and Huntsman 1992, 1995*a*).

Algal growth in iron- or zinc-limited phytoplankton is controlled by complex interactions among available metal concentration, cellular metal uptake rate, and intracellular metal concentration (Sunda and Huntsman 1995*a*,*b*; Sunda 2000). An inherent feedback exists between the specific growth rate and cellular metal, because the growth rate is directly related to the cellular concentration of limiting metal, whereas the cellular metal is inversely related to the specific growth rate, the effective rate of biodilution.

An additional controlling factor is the diel photoperiod, the duration of which regulates daily rates of carbon-fixation, growth, and cell division. Because photosynthesis occurs only during the day, the growth and composition of cells must vary over the diel cycle. Diel variations in cell carbon, carbohydrate, protein, chlorophyll *a* (Chl *a*), and major elemental ratios (e.g., nitrogen [N] : carbon [C], phosphorus [P] : C, and sulfur [S] : C) have been documented in cultured algae and natural phytoplankton growing under light/dark cycles (Hitchcock 1980; Owens et al. 1980; Cuhel et al. 1984; Vårum et al. 1986; Hama and Handa 1992; Burkhardt et al. 1999). Similar variations in cellular zinc and iron should also occur, but have not been previously examined.

The diel cycle may also influence cellular iron concentrations through day–night differences in iron chelation, linked to photochemical redox cycling (Fig. 1). Rates of iron and zinc uptake by phytoplankton are controlled by the concentration of dissolved inorganic metal species or free metal ions, which are regulated in seawater by metal complexation to organic ligands (Sunda 1988/1989; Morel et al. 1991). For most trace metals, such as zinc, this complexation is unaffected by light. Many iron chelates, however, undergo photo-redox cycling, which increases the concentration of dissolved inorganic Fe(II) and Fe(III) species (referred to as [Fe′]) and thus increases algal iron uptake rates in the light (Fig. 1), as demonstrated for a number of marine algae, including our test species *Thalassiosira pseudonana* (Anderson and Morel 1982; Sunda and Huntsman 1995*b* and unpubl. data). By increasing daytime iron uptake rates, photo-redox cycling should influence diel patterns of cellular iron.

We conducted experiments with the coastal diatom *T. pseudonana* to determine the interactive influence of day length and limiting concentrations of Fe and Zn on specific

Acknowledgments

I thank Patrick Griffin for technical assistance and Wayne Litaker, Patricia Tester, and two anonymous reviewers for helpful comments. This paper was partially funded by a grant from the Office of Naval Research.

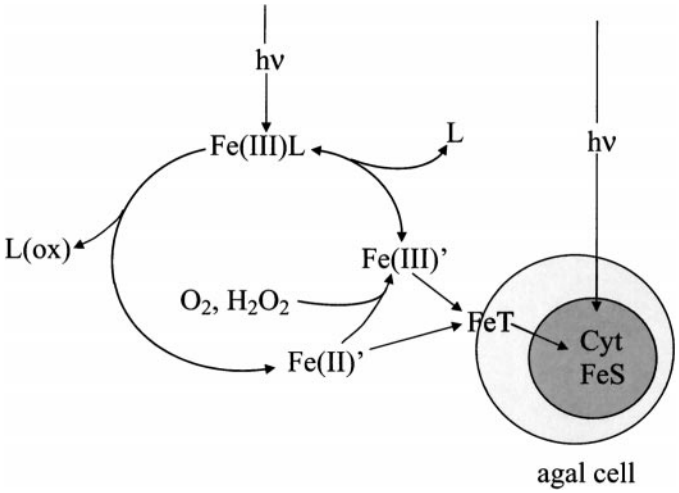

Fig. 1. Relationship between iron chemical dynamics and iron uptake by phytoplankton. Iron uptake is controlled by the reaction of inorganic Fe(II) species (Fe(II)′) and inorganic Fe(III) species (Fe(III)′) with transport proteins (T) on the outer cell membrane forming iron complexes with the proteins (FeT). The binding of iron to these uptake sites is related to the concentrations of Fe(II)′ and Fe(III)′. These concentrations, in turn, are determined by the balance between Fe(III)′ reaction with organic ligands (L; EDTA and NTA in our experiments) to form organic chelates (Fe(III)L) and dissociation of the chelates to reform Fe(III)′ and L. In the light, many ferric chelates such as Fe(III)EDTA absorb light (hν), which promotes an intramolecular charge transfer reaction in which the iron is reduced to Fe(II) and the ligand is oxidized to a degraded molecule, L(ox). The Fe(II) dissociates from the degraded ligand to form soluble Fe(II)′, which is subsequently oxidized by dioxygen (O_2) and hydrogen peroxide (H_2O_2) to re-form Fe(III)′. The reaction of Fe(III)′ with L to form Fe(III)L completes the iron photo-redox cycle. This cycle increases iron uptake by algal cells by increasing the steady-state concentrations of Fe(II)′ and Fe(III)′ species. The iron that is taken up by the cell is largely used to make cytochromes (Cyt) and iron–sulfur (FeS) redox centers necessary for photosynthetic and respiratory electron transport and for nitrate assimilation. The iron photo-redox cycle shown here and its influence on algal iron uptake are largely based on work by Anderson and Morel (1982) and Hudson and Morel (1990).

rates of C-fixation and growth and cellular concentrations of Chl *a*, fixed carbon, zinc, and iron. We also determined diurnal patterns in these constituents through repeated measurements throughout the light period. These patterns are influenced by day–night differences in specific rates of C-fixation and growth, which we quantified. The influence of iron photochemistry was also examined by measuring diurnal patterns in cellular iron in chelation regimes with contrasting levels of iron photo-redox cycling.

Materials and methods

Three growth and metal uptake experiments were conducted in acclimated cultures of *T. pseudonana* using previously described methods (Sunda and Huntsman 1992, 1995*a*,*b*). Experiments 1 and 2 examined the influence of limiting concentrations of zinc and iron, respectively, in cultures grown under a 7-h photoperiod (Table 1). The third experiment was conducted under a twofold longer photoperiod (14 h) and limiting iron conditions comparable to those utilized in one of the treatments in Experiment 2, thereby allowing us to determine day-length effects. In addition, this experiment examined the influence of photochemical cycling of iron by comparing results obtained in two different iron chelation regimes (*see below*).

An axenic culture of *T. pseudonana* (CCMP 1335, formerly clone 3H) was obtained from the Provasoli–Guillard Center for the Culture of Marine Phytoplankton (Bigelow Laboratory, Maine). It was maintained in f/8 medium (Guillard and Ryther 1962), using sterile technique, until needed. Experimental cultures were grown at 20°C and a pH of 8.2 ± 0.1 in 450-ml polycarbonate bottles containing 350 ml of seawater medium. They were grown under fluorescent lighting (Vita-Lite, Duro Test Corp.) at an intensity of ~500 μmol quanta m^{-2} s^{-1}. The experimental media consisted of filtered Gulf Stream seawater (salinity = 36) enriched with 32 μmol L^{-1} $NaNO_3$, 2 μmol L^{-1} Na_2HPO_4, 40 μmol L^{-1} Na_2SiO_3, 10 nmol L^{-1} Na_2SeO_3, 0.074 nmol L^{-1} vitamin B_{12}, 0.4 nmol L^{-1} biotin, and 60 nmol L^{-1} thiamin.

Trace metal ion buffer systems were added to quantify and control the concentrations of free trace metals ions or dissolved inorganic species, which regulate metal uptake by phytoplankton. The buffer system composition varied among the experiments. In Experiments 1 and 2, which examined zinc and iron limitation, respectively, the media contained 100 μmol L^{-1} of the chelator ethylenediaminetetraacetic acid (EDTA). The media in Experiment 1 contained a growth-saturating Fe concentration (1,000 nmol L^{-1}) and six Zn concentrations ranging from growth limiting to growth sufficient. In Experiment 2, the media contained two limiting concentrations of Fe (30 and 100 nmol L^{-1}) and a growth-sufficient concentration of Zn (100 nmol L^{-1}). Media in both experiments also contained growth-saturating concentrations of manganese (Mn) (50 nmol L^{-1}) and copper (Cu) (40 nmol L^{-1}). Cobalt was omitted in Experiment 1 because of its ability to nutritionally substitute for zinc (Sunda and Huntsman 1995*a*). In Experiment 2, cobalt was added at a concentration of 40 nmol L^{-1}.

Experiment 3 was conducted in two different iron chelation buffers: (1) 100 μmol L^{-1} EDTA and 100 nmol L^{-1} iron, a system in which photochemical redox cycling increases daytime Fe′ concentrations (and one of the iron treatments in Experiment 2), and (2) 500 μmol L^{-1} nitrilotriacetic acid (NTA) and 200 nmol L^{-1} iron, a treatment that yielded a similar mildly iron-limiting growth rate, but one in which there is no day/night difference in Fe′ concentration. A comparison of cultures grown in the two media allowed us to examine the effect of photochemical cycling on diurnal cellular iron patterns. Both buffer systems contained growth-saturating concentrations of other essential trace metals: 980 nmol L^{-1} Zn, 43 nmol L^{-1} Co, 171 nmol L^{-1} Mn, and 132 nmol L^{-1} Cu in the EDTA system and 65 nmol L^{-1} Zn, 3.3 nmol L^{-1} Co, 17 nmol L^{-1} Mn, and 12.6 nmol L^{-1} Cu in the NTA system. These concentrations yielded equivalent concentrations of free Zn, Co, Mn, and Cu ions in the two buffer systems (Table 2).

Free ion concentrations of Zn, Co, Mn, and Cu (Table 2) were computed from the total metal concentration and the

Table 1. Conditions and experimental results for the three long-term growth and metal uptake experiments.

Exp.	Light period (h)	Chelator (μmol L^{-1})	Total Fe (nmol L^{-1})	Log [Zn^{2+}]	Growth rate (d^{-1})	Growth rate (h $light^{-1}$)	C-fixation rate (h^{-1})	Cell Chl *a** (mmol L_{Cell}^{-1})	Cell volume* (μm^3)	Cell Zn or Fe* (μmol L_{Cell}^{-1})	Cell C† (mol L_{Cell}^{-1})
										Cell Zn	
1	7	100 EDTA	1,000	−12.00	0.73	0.104		5.76±0.11 (2)			
				−11.50	0.97	0.139	0.163	6.74±0.74 (4)	28.6±4.0	93±13 (2)	12.8±1.9
				−11.00	1.09	0.156	0.176	7.28±0.68 (4)	30.2±3.9	160±28 (2)	13.4±3.5
				−10.50	1.05	0.150	0.172	7.73±0.45 (4)	30.8±3.9	207±29 (2)	12.7±2.1
				−10.00	1.03	0.147	0.194	7.80±0.29 (4)	30.0±3.9	211±25 (2)	13.6±3.0
										Cell Fe	
2	7	100 EDTA	30	−10.99	0.59	0.084	0.108	4.52±0.51 (3)	23.6±2.5	430±26 (4)	15.5
			100	−10.99	0.88	0.126	0.178	5.82±0.62 (18)	29.5±3.1	650±61 (10)	15.0
3	14	100 EDTA	100	−10.00	1.50	0.107	0.133	3.25±0.50 (25)	37.2±1.8	495±54 (19)	16.0
		500 NTA	200	−10.00	1.58	0.133	0.148	3.29±0.65 (17)	37.8±2.6	576±43 (18)	16.0

* Mean ± SD ($n > 2$) or ±range ($n = 2$) for daylight values plotted in the figures. The number of observations is given in parenthesis.

† In Exp. 1, the mean ± range was computed for cell C concentration measured at the beginning and end of the light period. To determine daily mean cell C concentration in the second and third experiments, the mean cell C at each hour determined by linear regression (Figs. 3A, 4A) was summed and divided by the total number of hours. Values determined in this way are 5% higher than the simple mean of initial and final light period values, as computed for Exp. 1.

extent of metal complexation by EDTA or NTA and inorganic ligands, as determined from equilibrium calculations (Sunda and Huntsman 1992, 1995*a*). The computed ratios for free metal ion concentration to total metal in the 100 μmol L^{-1} EDTA media were $10^{-3.99}$ for Zn, $10^{-3.63}$ for Co, $10^{-1.23}$ for Mn, and $10^{-6.12}$ for Cu. NTA is a weaker chelator, and thus, the equivalent ratios were somewhat lower in the 500 μmol L^{-1} NTA media: $10^{-2.81}$ for Zn, $10^{-2.52}$ for Co, $10^{-0.24}$ for Mn, and $10^{-5.10}$ for Cu. This weaker chelation necessitated higher free Mn and Cu ion concentrations in Experiment 3 than used in Experiments 1 and 2 to maintain equivalent free ion concentrations of these metals in the EDTA and NTA buffer systems.

Computed concentrations of dissolved inorganic iron species ([Fe′]) in Fe–EDTA buffered media were computed from equilibrium or steady-state complexation relationships measured in the dark and under the same light regime used in our experiments (Sunda and Huntsman 2003). Based on these computations the [Fe′] is 3.5-fold to 5.7-fold higher in the light than in the dark in the EDTA media (Table 2). [Fe′] could not be computed for the NTA medium in Experiment 3 because of a lack of appropriate complexation data. However, experiments with both *Thalassiosira weissflogii* (Anderson and Morel 1982) and *T. pseudonana* (Sunda and Huntsman unpubl. data) show no increase in iron uptake in NTA media in the light, consistent with there being no photochemical increase in [Fe′]. The *T. pseudonana* experiments were conducted under the same light conditions used in the present experiments.

To initiate experiments, algal cells were transferred from f/8 media to experimental media containing the lowest or next-to-lowest concentration of the metal to be varied (i.e., [Zn^{2+}] = $10^{-11.5}$ mol L^{-1} in Experiment 1 and total iron concentrations of 30 and 100 nmol L^{-1}, respectively, in Experiments 2 and 3). The cells were acclimated in these media under the experimental light regime for seven to nine cell generations. They were then inoculated into two parallel sets of experimental media, one labeled with ^{14}C-bicarbonate to

Table 2. Computed concentrations of Fe′ and free ion concentrations of zinc (Zn), manganese (Mn), cobalt (Co), and copper (Cu) in the three culture experiments.

Exp.	Chelator (μmol L^{-1})	pH	Total Fe (nmol L^{-1})	[Fe′]* (pmol L^{-1}) Light	[Fe′]* (pmol L^{-1}) Dark	Log [Zn^{2+}]	Log [Co^{2+}]	Log [Mn^{2+}]	Log [Cu^{2+}]
1	100 EDTA	8.2±0.1	1,000	*	*	−12.00 to −10.00	~ −13.6	−8.53	−13.52
2	100 EDTA	8.20±0.06	30	137	34	−10.99	−11.03	−8.53	−13.52
		8.24±0.04	100	503	144				
3	100 EDTA	8.10±0.02	100	376	66	−10.00	−11.00	−8.00	−13.00
	500 NTA	8.08±0.03	200	*	*	−10.00	−11.00	−8.00	−13.00

* [Fe′] is the total concentration of dissolved inorganic ferric and ferrous species, [Fe(III)′] and [Fe(II)′], respectively. [Fe(III)′] in the EDTA media in Exps. 2 and 3 was computed from empirical steady-state (or equilibrium) ferric chelation data measured in the dark and under the same light regime as used in the present experiments (Sunda and Huntsman 2003). Values for [Fe(II)′] were determined from computed steady-state ratios of [Fe(III)′]/[Fe(II)′] based on Fe(II)′ oxidation kinetics and the photo-redox cycle shown in Fig. 1 (Sunda and Huntsman 2003). These ratios increase with pH and are 3.8, 6.0, and 7.2, respectively, at the experimental pH values of 8.10, 8.20, and 8.24. [Fe′] in Exp. 1 cannot be calculated because of precipitation of ferric hydroxides (Sunda and Huntsman 1995*b*). It also cannot be calculated in the NTA medium in Exp. 3 because of a lack of appropriate chelation data.

allow measurement of cellular fixed carbon and the other labeled with ^{59}Fe or ^{65}Zn (obtained from Amersham Radiochemicals) for measurement of cellular Fe or Zn. The cells were inoculated at biomass levels of 0.001–0.02 μl of cell volume per liter of culture and grown for 9–13 cell generations. Total cell concentrations and volumes were measured daily with a Coulter Multisizer II electronic particle counter.

To analyze for cell C, Fe, or Zn, exponentially growing cultures were filtered onto 2-μm pore Nuclepore filters at various times during the light period. Cellular fixed C was measured in ^{14}C-labeled cultures via liquid scintillation, and cellular Zn and Fe were determined in the ^{59}Fe- and ^{65}Zn-labeled cultures by gamma radiometry (Sunda and Huntsman 1995*a*,*b*). To measure intracellular iron, the filtered cells were exposed to a titanium–EDTA-citrate reducing solution for 2 min to reductively dissolve iron oxides and remove iron bound to cell surfaces (Hudson and Morel 1989). At each sampling time we also measured pH, cell Chl *a*, total cell numbers and cell volume per liter of culture, and average volume per cell (Sunda and Huntsman 1995*a*,*b*). The data were processed to give cellular concentrations of Zn, Fe, fixed C, and Chl *a* in units of moles per cell or per liter of cell volume. Chl *a* : C ratios were also computed for the ^{14}C-labeled cultures in which both Chl *a* and fixed carbon were measured. To compute cell Zn : C and Fe : C ratios, cell Zn or Fe concentrations were divided by cellular C concentrations measured at the same time of day in the parallel ^{14}C-labeled cultures.

In Experiment 1, a single set of measurements was made in each culture at the beginning and just past the end of the 7-h light period. However, in Experiments 2 and 3, a more extensive set of measurements was made throughout the light period over a 2- to 4-d period. These cultures were diluted periodically with fresh medium to maintain total cell volumes within a relatively narrow range (1–6 μl [L culture]$^{-1}$ in Experiment 2 and 0.8–2.4 μl [L culture]$^{-1}$ in Experiment 3). By doing this we prevented the growth of the cells from appreciably altering pH, nutrients, free metal ions, or CO_2.

To determine average daily growth rates, we regressed the natural log of total cell volume versus time over a 3–5-d period, after correcting for culture dilution with fresh medium (i.e., in Experiments 2 and 3). Data used for these regressions were collected at the same time of day. We also determined specific rates of C-fixation and growth during the day by regressing ln of the dilution-corrected fixed C concentration and total cell volume, respectively, versus time over a single light period. Specific growth rates in the dark (μ_D, in units of h^{-1}) were computed from the average daily specific growth rate (μ, d^{-1}) and the daytime specific growth rate (μ_L, h^{-1}) according to the equation

$$\mu_D = (\mu - \mu_L\, h_L)/h_D \quad (1)$$

where h_L and h_D are the hours of light and dark per day, respectively.

Results

Cell carbon, Chl a, *size, and growth rate*—The time of day, photoperiod, and growth rate limitation by iron or zinc all influenced the cellular concentrations of fixed C and Chl *a* and mean volume per cell. The diurnal patterns in these parameters showed some similarities and differences between the 7-h photoperiod (Experiments 1 and 2) and 14-h period (Experiment 3).

In Experiment 1, zinc limitation of growth rate occurred at zinc ion concentrations below 10^{-11} mol L^{-1} (Table 1). Zinc limitation was accompanied by decreases in cell Chl *a* concentration, but little effect was observed for cell C concentration or volume per cell (Table 1). The cell C concentration increased from a mean of 9.9 ± 0.4 mol per liter of cell volume (mol L_{cell}^{-1}) at the beginning of the light period to 16.3 ± 0.6 mol L_{cell}^{-1} at the end, a 65% increase (Fig. 2A). The average volume per cell increased by 30% (Fig. 2C), while the cellular Chl *a* concentration showed no variation ($P = 0.79$) (Fig. 2B).

In Experiment 2, cellular parameters were measured throughout the 7-h light period over 3–4 d in two iron-limited cultures. The intracellular iron and specific growth rate both increased as the iron concentration was increased from 30 and 100 nmol L^{-1} (Table 1). The specific growth rates (0.59 and 0.88 d^{-1}) were 56% and 83% of the maximum rate (~1.06 d^{-1}) under iron and zinc sufficiency. The volume per cell and cell Chl *a* concentration decreased with increasing iron limitation (as observed previously; Sunda and Huntsman 1995*b*), but the mean cellular carbon concentration showed little change (Fig. 3; Table 1).

Trends in cell C, Chl *a*, and volume per cell in Experiment 2 were similar to those in Experiment 1. At the higher iron level (100 nmol L^{-1}), the cell C concentration (mol L_{cell}^{-1}) increased linearly with time (h) and fit the equation

$$[\text{cell C}] = 1.39\ h + 10.5\ (R^2 = 0.92) \quad (2)$$

during the initial 80% of the photoperiod and then remained nearly constant for the remainder of the light period. Overall, the cell C concentration increased by 72% (from 10.5 to 18.1 mol L_{cell}^{-1}) over the 7-h light period. Decreasing iron to 30 nmol L^{-1} decreased the specific C-fixation rate (Table 1) and lowered the daytime percentage increase in [cell C] to 36% (Fig. 3A). There was no daytime trend in cell Chl *a* concentration (Fig. 3B), and volume per cell increased by 24% based on linear regression analysis (Fig. 3C).

In Experiment 3, conducted under a 14-h photoperiod, similar daily specific growth rates (1.50 and 1.58 d^{-1}) were observed in the two iron treatments (100 nmol L^{-1} Fe with 100 μmol L^{-1} EDTA and 200 nmol L^{-1} Fe with 500 μmol L^{-1} NTA) (Table 1). These rates are 83% and 88% of the maximum specific rate under iron sufficiency (~1.8 d^{-1}; Sunda and Huntsman 1995*b*). The percent of the maximum growth rate in the EDTA medium (83%) equals that observed for the same iron and EDTA treatment in Experiment 2 (*see above*).

Diurnal patterns in cell C, Chl *a*, and volume per cell in Experiment 3 were indistinguishable between the two iron treatments (Fig. 4). The cell C concentration increased linearly with time for the initial 80% (11 h) of the light period (Fig. 4A):

$$[\text{cell C}] = 0.79\ h + 10.5\ (R^2 = 0.91) \quad (3)$$

as in Experiment 2 under the same mild degree of iron lim-

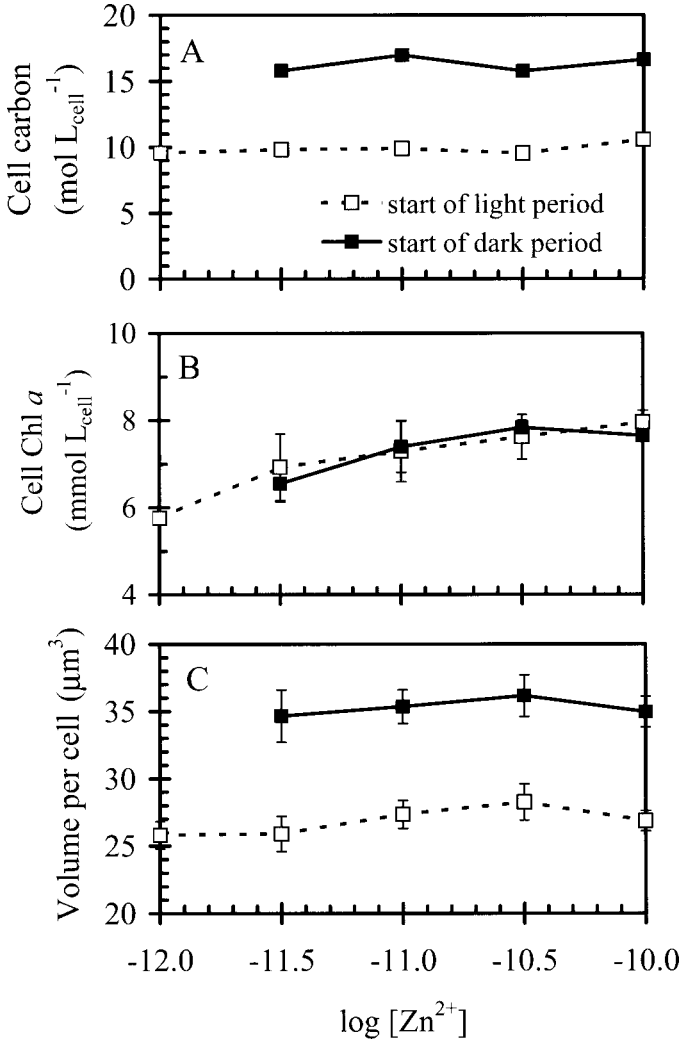

Fig. 2. Diurnal variations in (A) cellular carbon concentration (mol C per liter of cell volume), (B) cellular Chl *a* concentration (mmol per liter of cell volume), and (C) mean volume per cell. The data were collected at the beginning and end of a 7-h daily light period. They are plotted for free zinc ion concentrations ($[Zn^{2+}]$) ranging from growth limiting to growth saturating (*see* growth rate data in Table 1). Morning data only was collected for $[Zn^{2+}] = 10^{-12}$ mol L^{-1} because of a time constraint. Values for Chl *a* concentration and volume per cell are means ± range for duplicate cultures, one labeled with ^{14}C and the other with ^{65}Zn.

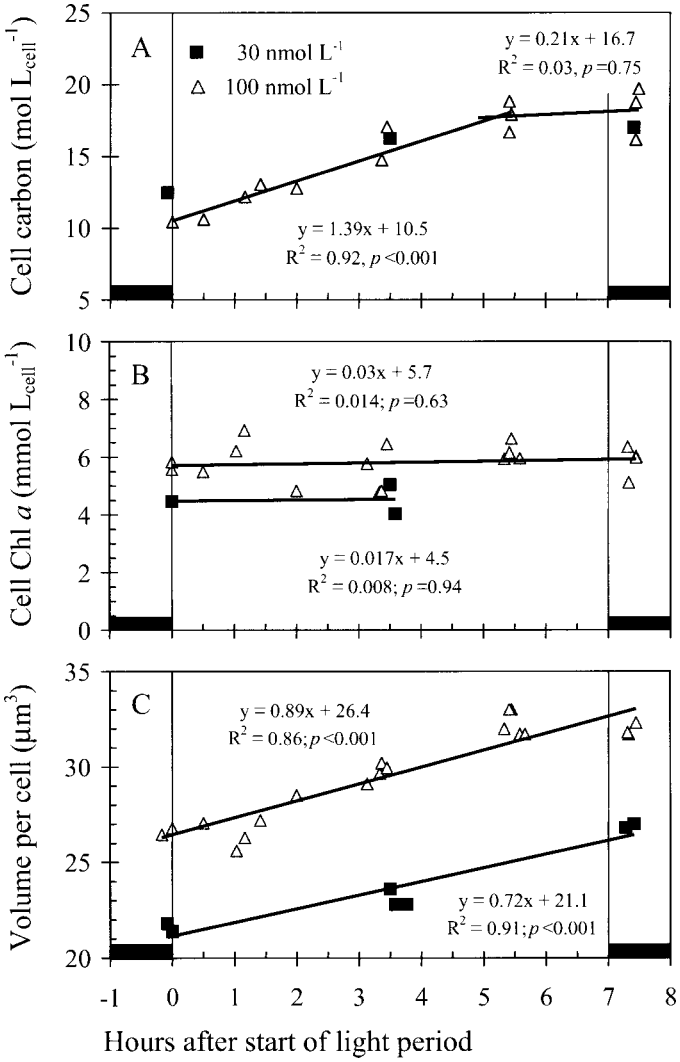

Fig. 3. Variations in (A) cellular fixed carbon concentrations, (B) cell Chl *a* concentrations, and (C) mean volume per cell during the 7-h light period in Experiment 2 conducted in EDTA media at iron concentrations of 30 and 100 nmol L^{-1}. Linear regression lines are shown. The data were collected over a 4-d period.

itation. The rate of increase was more gradual during the final 20% of the light period. A comparison with Eq. 2 shows that the cell C concentration at the start of the light period is the same for the two photoperiods, but the rate of increase is 72% higher for the 7-h period. This increase is apparently linked to the higher specific rate of C-fixation (Table 1). But because of its twofold longer duration, the 14-h photoperiod showed a higher percentage daytime increase in cell C concentration (96% vs. 72%). The daytime increase in cell C concentration reflects the fact that carbon is fixed photosynthetically only during the day and is lost to respiration at night (Fig. 5). Growth, as measured by the increase in total cell volume per liter of culture, occurs during both light and dark periods, albeit at a reduced rate in the dark (Fig. 5).

The diurnal patterns in cell Chl *a* and volume per cell observed over the 14-h light period in Experiment 3 differed from those for the shorter light period in Experiments 1 and 2. In Experiment 3, the volume per cell and cellular Chl *a* exhibited opposing sigmoidal patterns. The volume per cell increased during the morning, decreased during midday, and then increased again over the final 3 h of light (Fig. 4E), apparently reflecting diel cycles in cell division (Nelson and Brand 1979). The cell Chl *a* concentration showed an opposite pattern: it decreased slightly during the morning, increased during midday, and decreased again at the end of the light period (Fig. 4B). Chl *a*:C ratios and Chl *a* per cell also showed sigmoidal patterns, but their overall trends differed (Fig. 4C,D). Chl *a*:C trended downward during the day, reflecting the twofold increase in cell C concentration,

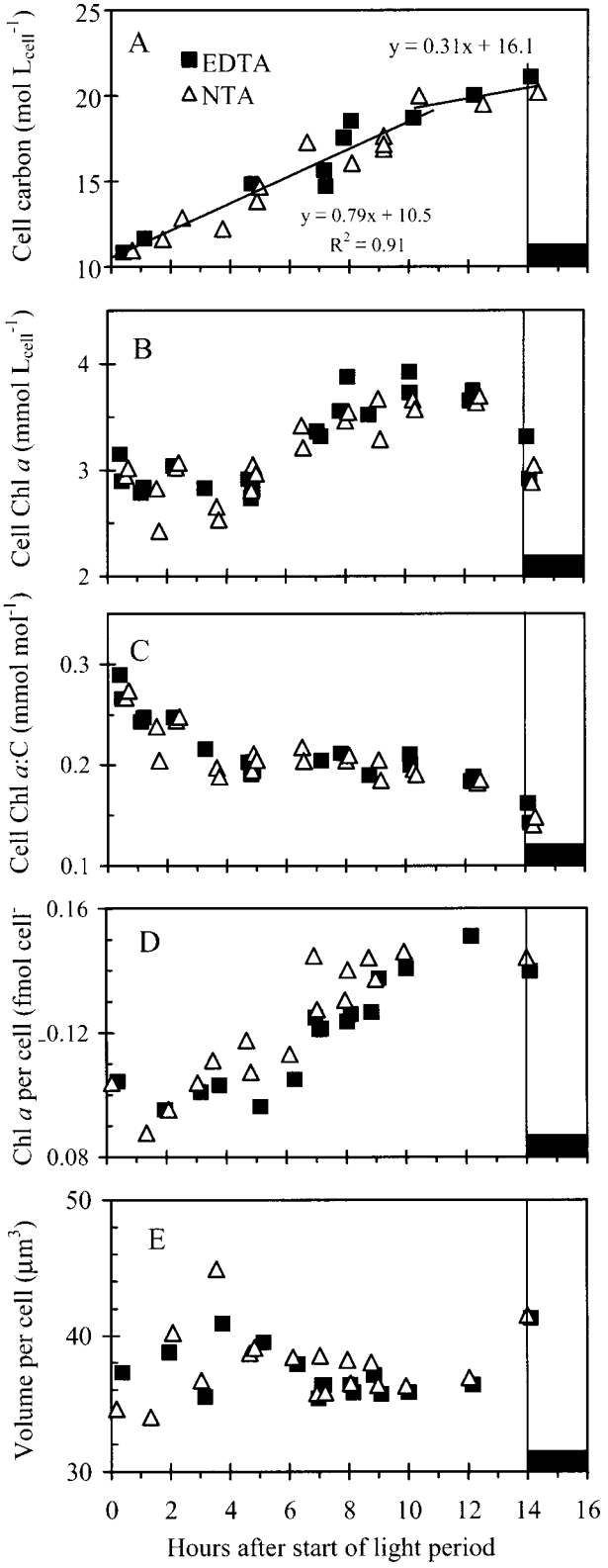

Fig. 4. Variations in (A) cellular fixed carbon concentrations, (B) cell Chl *a* concentrations, (C) cellular Chl *a*:C ratios, (D) Chl *a* per cell, and (E) mean volume per cell during the 14-h light period in Experiment 3 measured over a 2–4-d period. This experiment was conducted in two mildly iron-limiting media, one buffered with EDTA (100 μmol L^{-1} EDTA, 100 nmol L^{-1} iron) and the other with NTA (500 μmol L^{-1} NTA, 200 nmol L^{-1} iron).

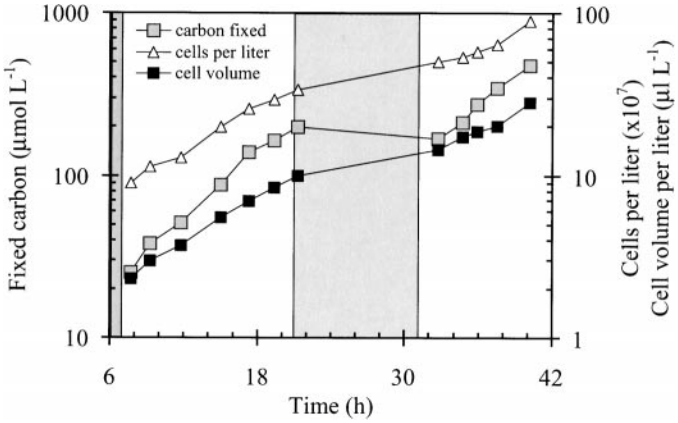

Fig. 5. Unbalanced growth in cellular fixed carbon, total cell volume, and cells per liter of culture during successive light and dark periods in the EDTA medium in Experiment 3. The three virtual growth curves were constructed by factoring out the effects of culture dilution with new medium. Carbon is fixed only in the light, and its rate of increase in the light is substantially higher than that for cell volume, resulting in a twofold daytime increase in cell C concentration (*see* Fig. 3A).

whereas Chl *a* per cell trended upward. Thus, the overall daytime pattern in cellular Chl *a* depends on which parameter (cell volume, cell C, or cell numbers) it was normalized to.

Relationships among photoperiod, Chl a, *cellular Fe : C, and specific rates of C fixation and growth*—Decreasing the photoperiod from 14 h (Experiment 3) to 7 h (Experiments 1 and 2) decreased the daily specific growth rate, increased the average cellular iron and Chl *a* concentrations, and increased the specific photosynthetic C-fixation rate in nonlimited or mildly iron- and zinc-limited cultures (Table 1). In the mildly Fe-limiting treatment with 100 μmol L^{-1} EDTA and 100 nmol L^{-1} Fe, the halving of the photoperiod decreased the specific growth rate by 41% and increased the mean cellular iron and Chl *a* concentrations by 31% and 79%, respectively. There was an associated 34% increase in the daytime specific C-fixation rate (Table 1).

In the iron experiments (Experiments 2 and 3), the specific C-fixation rate followed a single linear relation with the intracellular Fe : C ratio, regardless of the photoperiod (Fig. 6). The slope of this relationship, 4,200 mol C h^{-1} (mol Fe)$^{-1}$, defines the marginal iron use efficiency (MIUE), the moles of additional cellular C fixed per hour per additional mole of intracellular Fe. This value compares with a calculated MIUE of 3,100 mol C (mol Fe)$^{-1}$ h^{-1} based on the metabolic iron needed to support photosynthetic electron transport (PET), nitrate reduction, and respiratory electron transport (Raven 1988). The calculations assume a 1 : 1 : 1 : 1 : 1 stoichiometry for iron-containing PET components (photosystem II, cytochrome b_6-f complex, cytochrome c, photosystem II, and ferredoxin), yielding a total of 23 iron atoms per PET chain (Raven et al. 1999). The agreement between observed and modeled MIUE values is reasonable given the uncertainties in the model calculations and the fact that the

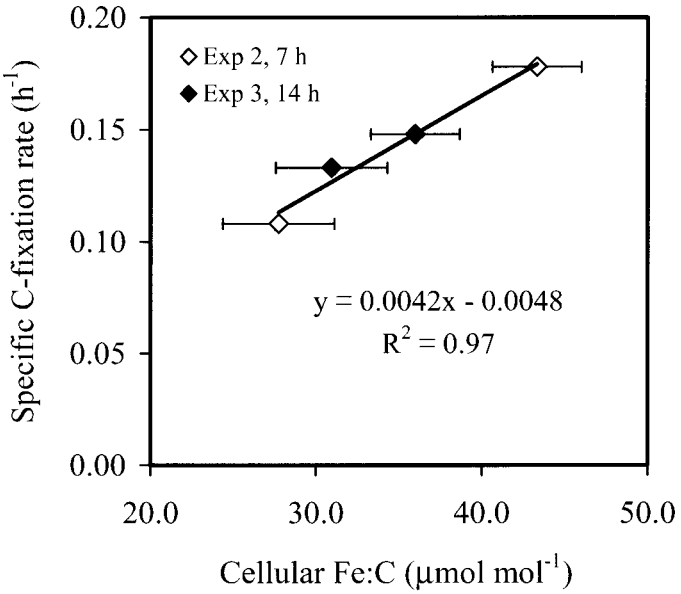

Fig. 6. Relationship between the net specific C-fixation rate and the intracellular Fe : C ratio in Experiments 2 and 3. The linear regression equation, line, and R^2 are given. Error bars give standard deviations.

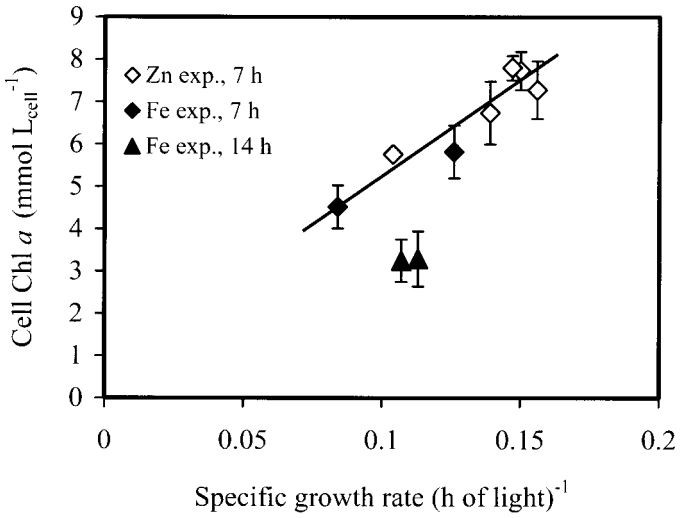

Fig. 7. Relationship between mean daytime cellular Chl *a* concentration and daily specific growth rate divided by hours of light per day. Data are plotted for the two 7-h photoperiod experiments with varying zinc and iron limitation and for the 14-h photoperiod experiment under mildly iron-limiting conditions. The data are taken from Table 1.

calculations assume balanced cell growth under continuous light (Raven 1988, 2000).

In the two 7-h photoperiod experiments, the cellular Chl *a* concentration ([cell Chl *a*]) showed a single linear relationship with specific growth rate under both zinc and iron limitation (Fig. 7):

$$[\text{cell Chl } a] = 42.9\ \mu_{hl} + 0.97\ (R^2 = 0.89) \qquad (4)$$

In Eq. 4, μ_{hl} is the daily specific growth rate divided by the daily hours of light (i.e., by the hours of photosynthetic C fixation), and 0.97 mol L_{cell}^{-1} is the extrapolated [cell Chl *a*] at zero growth rate.

Because growth is dependent on C-fixation, values of μ_{hl} and specific C-fixation rate were closely correlated in all three experiments (linear regression $R^2 = 0.83$). In exponentially growing cells, the daily specific growth rate divided by the hours of light should equal the hourly net specific C-fixation rate minus nighttime losses of cell carbon, primarily to respiration. In our experiments, these rates were 80 ± 6% of net C-fixation rates (Table 1), indicating an ~20% nighttime cellular loss of fixed carbon. This value agrees with that (19 ± 4%) measured in cultures of *T. weissflogii* (formerly *T. fluviatilis*) grown on a 6 : 18-h light : dark cycle (Hobson et al. 1985).

Variations in cellular zinc—In Experiment 1, mean cellular zinc concentrations increased at zinc ion concentrations ($[Zn^{2+}]$) up to ~$10^{-10.5}$ mol L^{-1} and approached a constant value of ~200 μmol L_{cell}^{-1} at higher $[Zn^{2+}]$ (Table 1). Cellular zinc varied over the 7-h light period, and the amount of variation depended on how cell zinc was expressed. The cell zinc concentration (normalized to cell volume) decreased by an average of 25 ± 4% during the light period (Fig. 8A), owing to a higher specific rate of cell volume increase during the day (~2.1 d^{-1}) than at night (~0.6 d^{-1}), and resulting higher daytime biodilution rate (Fig. 9). Cell Zn : C ratio decreased by an even larger percentage (54 ± 4%) (Fig. 8B), reflecting the combined effect of the 25% decrease in cell Zn concentration and 64 ± 4% increase in cell C concentration (Fig. 2A). Finally, the zinc per cell showed no change ($P = 0.95$)(Fig. 8C) because the 25% daytime decrease in zinc per unit of cell volume was effectively canceled by the 30% increase in volume per cell.

Diurnal variations in cellular iron—Diurnal variations in cellular iron are influenced not only by day–night differences in growth processes but also by changes in iron availability caused by photo-redox cycling (Fig. 1), which should increase daytime iron uptake rates in the EDTA media in Experiments 2 and 3. In Experiment 2, there was no trend in cellular iron concentration during the 7-h photoperiod (Fig. 10A), contrasting with the previous results for zinc. For iron, the increased biodilution during the day (which tends to decrease cellular metal concentration) apparently was cancelled by an increased rate of iron uptake due to photochemical redox cycling. Cellular Fe : C ratios in Experiment 2 decreased during the day (Fig. 10B), and the percentage decrease was threefold greater at the higher iron concentration, reflecting the higher percentage increase in cell C concentration (Fig. 3A). Iron per cell followed the opposite trend and increased over the 7-h photoperiod (Fig. 10C). Thus, daytime trends in cellular iron differ from those of zinc, but like Chl *a* and zinc, the exact pattern depends on which cellular parameter it is normalized to.

The effect of photo-dissociation of Fe-chelates was further investigated in Experiment 3 by comparing diurnal variations in cellular iron in EDTA media, where photochemical cycling increases the daytime Fe′ concentration, with variations in NTA media, where no photochemical change in

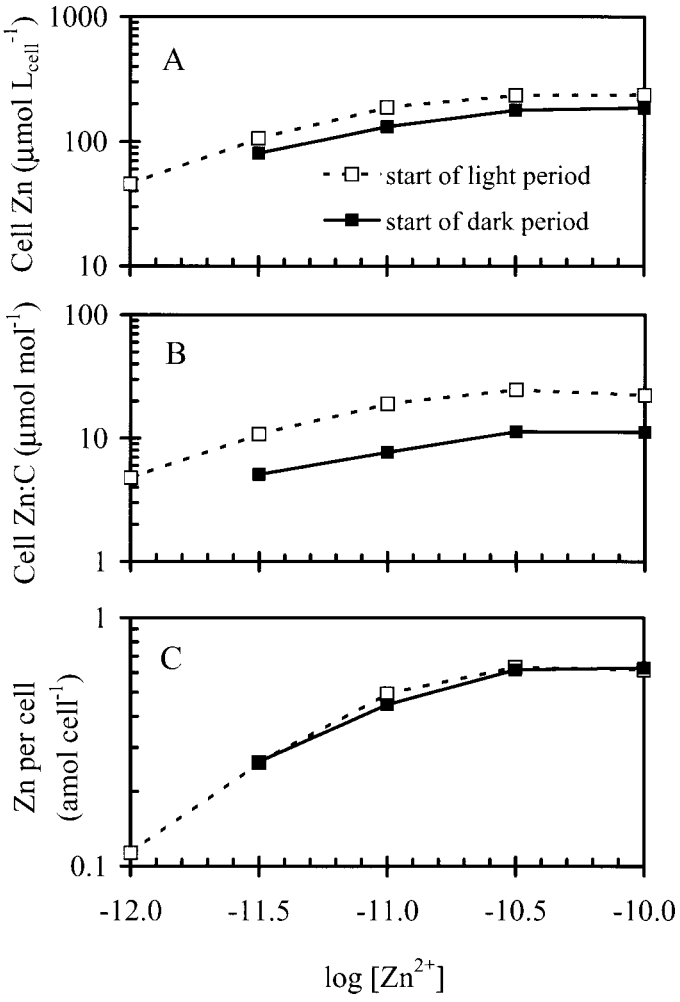

Fig. 8. Diurnal variations in (A) cellular Zn concentration, (B) cellular Zn : C ratio, and (C) Zn per cell in Experiment 1 for free zinc ion concentrations ranging from growth limiting to growth saturating (*see* Table 1).

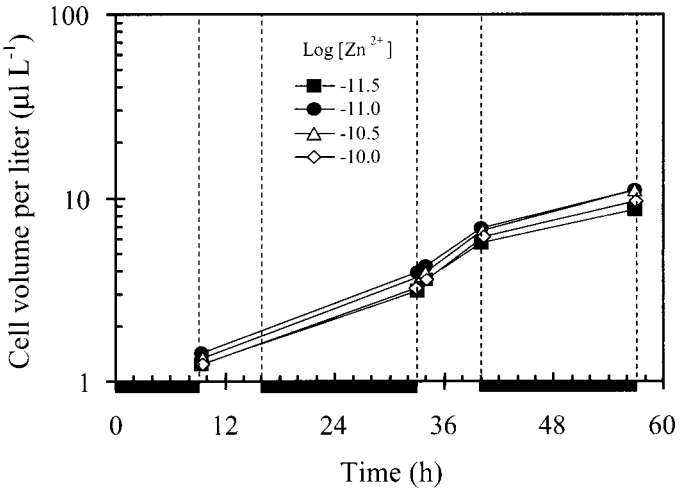

Fig. 9. Increase in total cell volume per liter of culture during light and dark periods for cells grown on a 7 : 17-h light : dark cycle in Experiment 1. Average growth rates in the light were ~2.1 d^{-1}, while those in the dark were ~0.6 d^{-1}, yielding an average daily growth rate of ~1.0 d^{-1}.

Fe′ occurs. The cellular iron concentration showed quite different daytime trends depending on the choice of chelator. It increased in the EDTA medium, apparently owing to the large daytime increase in [Fe′], but it decreased in the NTA medium (Fig. 11A). The increase in cellular iron concentration in the EDTA medium in Experiment 3 contrasts with the lack of daytime trend in Experiment 2. This difference in trends is likely accounted for by the higher relative increase in [Fe′] during the day versus the night in Experiment 3 (5.7-fold) compared to that in Experiment 2 (3.5-fold), resulting from a lower pH (Table 2; *see* Sunda and Huntsman 2003). When cellular iron was normalized to carbon in Experiment 3, the resulting cell Fe : C ratios decreased in both the EDTA and NTA media, but the rate of decrease in the NTA medium was three times higher than that in the EDTA medium (Fig. 11B).

Discussion

Diel variations in growth and cell C concentration—Under nutrient limitation (e.g., by Fe or Zn), the specific rates of C-fixation and growth, the cellular concentrations of nutrient element and Chl *a*, and the uptake rate of the nutrient are all integrally linked (Sunda and Huntsman 1997; Sunda 2001). Furthermore, the functional relationships among these variables change with the length of the photoperiod, which provides a fundamental control on daily rates of C-fixation.

The existence of the photoperiod leads to large diel differences in net rates of C-fixation and growth and in cell C concentration. In our experiments, we observed 64% to 96% daytime increases in cell C concentration for cells growing at or near their maximum rates. The increase reflects C-fixation during the day and partial storage as carbohydrates (e.g., β-1,3-D-glucan; Vårum et al. 1986). This stored carbon is then utilized during the dark period to support respiration, protein synthesis, and growth (Cuhel et al. 1984). A combination of respiratory carbon consumption and cell volume increases due to growth causes cell carbon concentrations to decrease during the night, completing the diel cycle.

Our cell volume data show that cellular growth rates are reduced at night (Figs. 5, 9). At the four highest zinc ion concentrations in Experiment 1, the average daily specific growth rate was 1.03 ± 0.05 d^{-1}, and the specific rate during the 7-h light period was 0.084 ± 0.006 h^{-1}, yielding a computed rate of 0.026 ± 0.001 h^{-1} during the 17-h dark period (*see Eq. 1*). Based on these data, 57% of the cell volume–based growth occurred during the day. In the EDTA treatment in Experiment 3, the specific growth rates in the light and the dark were 0.087 and 0.028 h^{-1}, respectively, and the overall daily rate was 1.50 d^{-1}. Here a higher percentage (81%) of the volume-based growth occurs during the day owing to the longer 14-h photoperiod.

Photo-acclimation to decreasing photoperiod—To support a higher percentage of nighttime growth, cells acclimated to the shortened (7-h) photoperiod must store substantial amounts of fixed carbon during the day. This storage requires a high rate of photosynthetic C-fixation, given the

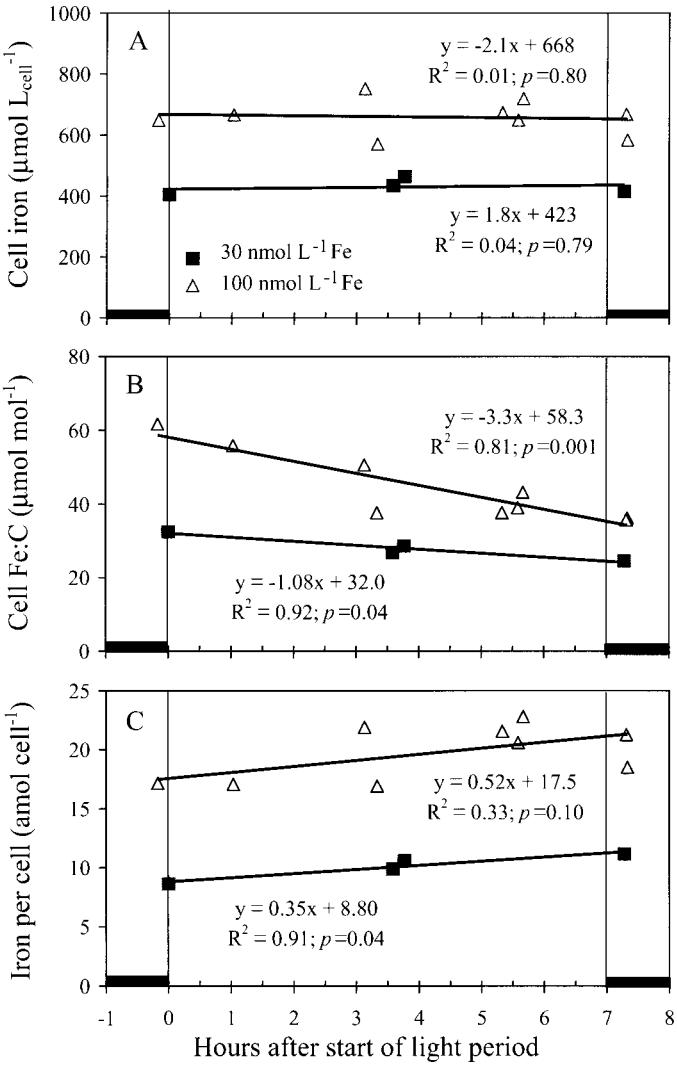

Fig. 10. Variations in (A) intracellular iron concentration, (B) cellular Fe : C ratio, and (C) iron per cell during the 7-h light period in Experiment 2 conducted in EDTA media at two growth-limiting iron concentrations (30 and 100 nmol L^{-1}). Linear regression lines are shown.

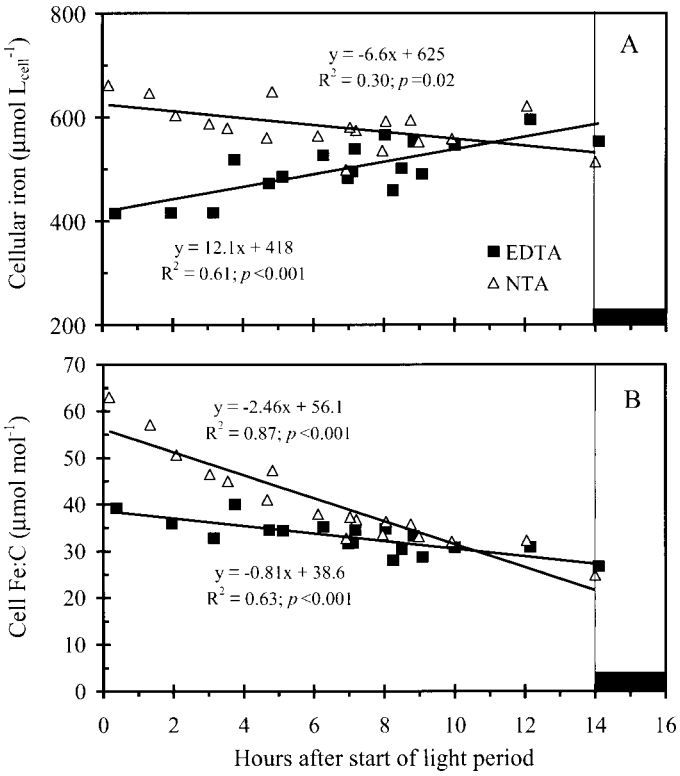

Fig. 11. Variations in (A) intracellular Fe concentration, (B) cellular Fe : C molar ratio in Experiment 3 conducted in mildly iron-limiting EDTA (100 μmol L^{-1} EDTA, 100 nmol L^{-1} iron) and NTA (500 μmol L^{-1} NTA, 200 nmol L^{-1} iron) media. Linear regression lines are shown.

short duration of the photoperiod. This indeed is what we observed. Cells grown at 100 nmol L^{-1} iron in EDTA medium had a 34% higher specific net C-fixation rate under a 7-h photoperiod than they did under a 14-h period (Table 1). Similar increases in photosynthetic C-fixation rate with decreasing photoperiod have been observed in *T. weissflogii* (Hobson et al. 1985). In this species, the midday short-term C-fixation rate per cell increased by a 2.7-fold as the photoperiod was decreased from 18 to 6 h.

Based on our present and previous experimental results (Fig. 6; Sunda and Huntsman 1997) and molecular iron use efficiency models (Raven 1988, 1990), an increase in specific C-fixation rate under iron limitation requires an increase in cellular Fe. Such an increase in fact is observed. In the two Fe-limited cultures containing EDTA and 100 nmol L^{-1} Fe, cells grown under the shorter photoperiod had a 40% higher mean daytime Fe : C ratio (Table 1), sufficient to support the 34% higher net C-fixation rate. Based on molecular models, roughly half of the metabolic iron is needed for photosynthetic reaction centers and associated electron transport proteins, while the remainder is needed for synthesis of nitrate and nitrate reductase enzymes and components of the respiratory electron transport chain (Raven 1988; Raven et al. 1999).

The increased photosynthetic C-fixation rate observed under a shortened light period represents a photo-acclimation, resembling in part that occurring under low light intensity. Acclimation to low irradiance largely involves an increase in photosynthetic capacity (and thus an increase in cellular Fe) to partially compensate for the undersaturated state of the photosynthetic apparatus with respect to light (Raven 1990). Iron-limited phytoplankton cells cannot obtain this additional iron by increasing their iron uptake rates, as these rates appear to already operate at their physical and chemical limits (Hudson and Morel 1990; Sunda and Huntsman 1995*b*, 1997). The cellular iron concentration is directly related to the uptake rate and inversely related to the specific growth rate (see Eq. 5 below). Consequently, the reduced growth rate under low irradiance allows the cells to accumulate the increased iron needed for synthesis of additional photosynthetic units (Sunda and Huntsman 1997). The same dynamic appears to be at play in the iron-limited cultures in the present experiments, but here it is the shortened photo-

period and resultant decrease in growth rate that provide for the necessary increase in cellular iron.

Consistent with the increased photosynthetic C-fixation rate, a decrease in the photoperiod was accompanied by higher cell Chl *a* concentrations (Table 1). Similar increases in Chl *a* with decreasing day length have been observed for other algal species and have been generally attributed to a photo-acclimation (Terborgh and Themann 1964; Hobson et al. 1979, 1985; Verity 1981; Sakshaug and Andersen 1986; Nielsen 1992).

Balancing light capture and growth—Under constant day length and varying levels of iron and zinc limitation, cellular Chl *a* concentrations decreased as a linear function of specific growth rate. A similar linear relationship between Chl *a*:C ratio and specific growth rate has been observed in the coastal diatom *Skeletonema costatum* under varying levels of nitrogen limitation (Sakshaug et al. 1989). Likewise, total Chl (Chl *a* + Chl *b*) was linearly correlated with the light-saturated C-fixation rate in iron-limited terrestrial plants (Terry 1980). Decreases in Chl *a* under iron limitation have been widely reported in algae and terrestrial plants and have been historically attributed to a metabolic requirement for iron in Chl *a* synthesis (Karali and Price 1963). However, such a mechanism does not readily explain the virtually identical relationship between Chl *a* and specific growth rate that we observed under zinc limitation, as Zn is not known to be directly involved biochemically in Chl *a* synthesis. Alternatively, the decrease in Chl *a* under iron limitation has been proposed to be fundamentally linked to the decrease in the synthesis of photosynthetic units resulting from a decrease in the supply of iron for synthesis of critical iron-containing components of these units, namely iron–sulfur redox centers and cytochromes (Spiller and Terry 1980; Sunda and Huntsman 1997). Ultimately, plants must maintain a balance among sequentially linked photosynthetic and biosynthetic processes: light capture by Chl *a* and other pigments, charge separation within photosynthetic reaction centers, electron transfer to NADP, CO_2 fixation in the Calvin–Bensen cycle, and subsequent synthesis of essential biomolecules (e.g., proteins). Molecular studies have revealed that cells regulate the capacity and composition of the photosynthetic apparatus by sensing the redox state of key components of the photosynthetic electron transport chain, such as the plastiquinone pool or the b_6-*f* complex (Escoubas et al. 1995; Pfannschmidt 2003). Any nutrient limitation that restricts metabolic and biosynthetic processes downstream of light capture by Chl *a* should elicit a downregulation of the photosynthetic system, and thus Chl *a* levels, to restore the balance between light capture and biosynthesis (Kana et al. 1997). According to this view, the nature of the limitation is less significant than its overall effect in limiting rates of C-fixation and growth.

Photoperiod effects on cellular metal—The cellular metal content in phytoplankton is determined by the balance between rates of metal uptake and dilution by growth. In acclimated exponentially growing cells, the daily average cellular metal concentration and average specific rates of metal uptake (V_{ss}) and growth (μ) typically do not vary from day to day and, thus, can be considered to be at steady state. Consequently, they conform the steady-state equation

$$[\text{cell metal}] = V_{ss}/\mu \quad (5)$$

But because the specific growth rate varies with time of day and because the cellular metal uptake rate may also vary depending on diel changes in external chemistry and cell energetics, the cellular metal concentration usually also varies over the diel cycle. As we have shown, the specific growth rate (based on cell volume) is often considerably higher during the day than at night, and if the uptake rate is similar for both periods, then the cellular nutrient metal concentration will decrease during the day, as observed for zinc in Experiment 1 and for iron in the NTA buffered medium in Experiment 3. The relative decrease in cellular metal:C ratios is even greater because of the daytime increase in cellular C concentration. Thus, in Experiment 3, the cellular Fe concentration in the NTA medium decreased by ~23% during the day based on the linear regression analysis, but the Fe:C ratio decreased by 63%, or 2.7-fold (Fig. 11).

The relative change in the cellular metal concentration or metal:C ratio should decrease with decreasing specific rates of C-fixation and growth, as observed in Experiment 2 under increasing levels of Fe-limitation. As a corollary to this, larger cells, which typically exhibit lower growth rates under a given set of limiting nutrients (Sunda and Huntsman 1997), should also show lower daytime decreases in cellular metal concentrations and metal:C ratios.

An additional factor for iron is photo-redox cycling, which increases its availability during the day by increasing the steady-state concentration of biologically available inorganic Fe(II) and Fe(III) species (Fig. 1). For iron, the direction of the daytime change in cellular metal is determined by the relative day–night variations in cellular metal uptake rate and specific growth rate. The cellular metal concentration may increase, decrease, or remain the same depending on the magnitude of these relative diel variations, and indeed, all three patterns are observed in our experiments. If the iron uptake rate and the specific growth rate increase by similar degrees between night and day, as appears to have occurred in Experiment 2, then the cellular metal concentration will be independent of time of day. If, on the other hand, the specific growth rate increases by more than the iron uptake rate (as in the NTA medium in Experiment 3), then the cellular iron will decrease during the day; and if the uptake rate increases more than the specific growth rate (as likely occurred in the EDTA medium in Experiment 3), then the cellular iron concentration will increase. However, as carbon is fixed by photosynthesis only during the day and is lost to respiration at night, the Fe:C ratio should always decrease during the light period, as was again observed in all of our iron experiments. The rate of decrease will be much lower in situations in which there is a substantial increase in daytime iron uptake due to photo-redox cycling, as observed in Experiment 3 (Fig. 11B).

There is strong evidence for substantial photo-redox cycling of iron in seawater, although its exact effect on iron uptake by phytoplankton has not yet been established (Sunda 2001). Photo-redox cycling of iron has been observed in seawater from the northeast coast of the United States (Mill-

er et al. 1995), shelf waters off northern Australia (Waite et al. 1995), and in equatorial Pacific water amended with added iron (Johnson et al. 1994). Iron is heavily chelated in seawater by strong organic ligands with stability constants close to those for bacterial siderophores, indicating that many of these ligands may be siderophores (Rue and Bruland 1997). Recently, iron chelates with marine bacterial siderophores were shown to undergo photo-redox cycling when exposed to solar radiation, and this cycling substantially increased iron uptake by a coastal diatom (Barbeau et al. 2001). In the ocean, the photolysis of iron-siderophores or other iron complexes may substantially increase daytime iron uptake rates by phytoplankton and thereby influence diel patterns in cellular iron concentrations and Fe : C ratios.

Diurnal variations and their implications—The diel variation in cellular concentrations of metals, fixed carbon, and other constituents have several important implications. A first relates to zooplankton feeding behavior. Feeding in late afternoon or early evening, when cellular carbon concentrations are highest, will allow a zooplankter to maximize its carbon intake, and indeed, many vertically migrating zooplankton largely feed during this time. However, whether they employ this feeding strategy in part to optimize their nutrition remains an open question.

A second implication relates to optimal sampling strategies in algal culture experiments conducted under light/dark cycles. It is clear that the value of a given cellular parameter often depends on the time of day during which it was measured. Although culturists have realized this truism for some time, they have not always practiced the best sampling strategy. Often in a large experiment, there is time only for one sampling per day, and in these cases, it is probably best to sample during the middle of the light period, when cellular parameters are at or close to their average daily values. This strategy allows for a more valid comparison of cell composition of phytoplankton growing at different specific rates or under different photoperiods. Average cell values are also necessary for computing daily metal uptake rates (V_{ss}) from cellular metal concentration and specific growth rate (μ) in acclimated, exponentially growing cultures:

$$V_{ss} = \mu[\text{cell metal}] \quad (6)$$

This equation is a rearrangement of Eq. 5, and as noted previously, it is valid only for average daily values of V_{ss}, μ, and [cell metal] under diel light cycles.

A third implication relates to the measurement of cellular concentrations of metals, carbon, and metal : carbon ratios in field samples of marine algae and particulate matter, the latter often being dominated by phytoplankton cells. The time of day is typically not considered in such sampling and often is not even mentioned for published data. Variations in phytoplankton or particulate composition measured along transects that are attributed to sample location might in part result from the time of day of sampling. Although it is usually impossible in a field situation to collect all samples at the same time of day, there nonetheless needs to be a recognition among field biologists and chemists that metal concentrations and metal : C ratios in marine phytoplankton often vary with time of day.

A final implication relates to algal Fe : C ratios in oceanic carbon cycling models, which are used to predict air–sea exchange of CO_2 and, thus, atmospheric CO_2 inventories and future changes in global climate. As initially proposed by Martin and Fitzwater (1988), iron is now known to be an important limiting factor for oceanic productivity (Coale et al. 1996; Boyd et al. 2000), which regulates the removal of CO_2 from surface ocean waters and its transport to the deep ocean, the so-called biological CO_2 pump. A significant issue in carbon sequestration models is the Fe : C ratio in phytoplankton, which provides a fundamental control on the moles of carbon that can be fixed and transported to the deep ocean per mol of available iron (Moore et al. 2002). Our data indicate that Fe : C ratios can vary substantially in phytoplankton with time of day (by up to a 2.7-fold in *T. pseudonana*) and photoperiod, and such variations may influence carbon transport rates. For example, much of the transport of particulate carbon to the deep sea is linked to zooplankton grazing and the production of rapidly sinking fecal pellets (Moore et al. 2002). Many zooplankton vertically migrate to the surface at the end of the light period, when algal fixed carbon levels and C : Fe ratios are at their highest daily values. Such preferential grazing during this period may increase the C : Fe ratios in settling fecal material and thus heighten the removal of CO_2 for a given amount of available iron. This effect may be mitigated by the fact that the export of fixed carbon to the deep ocean is primarily associated with large cells, which may have lower diel variations in C : Fe ratios because of their lower specific growth rates. Such diel effects nonetheless may still need to be considered in refining oceanic carbon cycling models.

References

ANDERSON, M. A., AND F. M. M. MOREL. 1982. The influence of aqueous iron chemistry on the uptake of iron by the coastal diatom *Thalassiosira weissflogii*. Limnol. Oceanogr. **27:** 789–813.

BARBEAU, K., E. L. RUE, K. W. BRULAND, AND A. BUTLER. 2001. Photochemical cycling of iron in the surface ocean mediated by microbial iron(III)–binding ligands. Nature **413:** 409–413.

BOYD, P. W., AND OTHERS. 2000. A mesoscale phytoplankton bloom in the polar Southern Ocean stimulated by iron fertilization. Nature **407:** 695–702.

BRAND, L. E., W. G. SUNDA, AND R. R. L. GUILLARD. 1983. Limitation of marine phytoplankton reproductive rates by zinc, manganese and iron. Limnol. Oceanogr. **28:** 1182–1198.

BURKHARDT, S., I. ZONDERVAN, AND U. RIEBESELL. 1999. Effect of CO_2 concentration on C:N:P ratio in marine phytoplankton: A species comparison. Limnol. Oceanogr. **44:** 683–690.

Coale, K. H. 1991. Effects of iron, manganese, copper, and zinc enrichments on productivity and biomass in the subarctic Pacific. Limnol. Oceanogr. **36:** 1851–1864.

——— AND OTHERS. 1996. A massive phytoplankton bloom induced by an ecosystem-scale iron fertilization experiment in the equatorial Pacific Ocean. Nature **383:** 495–501.

CUHEL, R. L., P. B. ORTNER, AND D. R. S. LEAN. 1984. Night synthesis of protein by algae. Limnol. Oceanogr. **29:** 731–744.

ESCOUBAS, J., M. LOMAS, J. LA ROCHE, AND P. G. FALKOWSKI. 1995. Light intensity regulation of *cab* gene transcription is signaled by the redox state of the plastoquinone pool. Proc. Natl. Acad. Sci. USA **92:** 10237–10241.

GUILLARD, R. L., AND J. H. RYTHER. 1962. Studies of marine plankton diatoms, I. *Cyclotella nana* Hustedt, and *Detonula confervacea* (Cleve) Gran. Can. J. Microbiol. **8:** 437–445.

HAMA, J., AND N. HANDA. 1992. Diel variations of water-extractable carbohydrate composition of natural phytoplankton populations in Kinu-ura Bay. J. Exp. Mar. Biol. Ecol. **162:** 159–176.

HITCHCOCK, G. L. 1980. Diel variations in chlorophyll *a*, carbohydrate, and protein content of the marine diatom *Skeletonema costatum.* Mar. Biol. **57:** 271–278.

HOBSON, L. A., F. A. HARTLEY, AND D. E. KETCHAM. 1979. Effects of variations in daylength and temperature on net rates of photosynthesis, dark respiration, and excretion by *Isochrysis galbana* Parke. Plant Physiol. **63:** 947–951.

———, W. J. MORRIS, AND K. P. GUEST. 1985. Varying photoperiod, ribulose 1,5-bisphosphate carboxylase/oxygenase, and CO_2 uptake in *Thalassiosira fluviatilis* (Bacillariophyceae). Plant Physiol. **79:** 833–837.

HUDSON, R. J. M., AND F. M. M. MOREL. 1989. Distinguishing between extra- and intracellular iron in marine phytoplankton. Limnol. Oceanogr. **34:** 1113–1120.

———, AND ———. 1990. Iron transport in marine phytoplankton: Kinetics of cellular and medium coordination reactions. Limnol. Oceanogr. **35:** 1002–1020.

HUTCHINS, D. A., G. R. DiTULLIO, Y. ZHANG, AND K. W. BRULAND. 1998. An iron limitation mosaic in the California upwelling regime. Limnol. Oceanogr. **43:** 1037–1054.

JOHNSON, K. S., K. H. COALE, V. A. ELROD, AND N. W. TINDALE. 1994. Iron photochemistry in seawater from the equatorial Pacific. Mar. Chem. **46:** 319–334.

KANA, T. M., R. J. GEIDER, AND C. CRITCHLEY. 1997. Regulation of photosynthetic pigments in micro-algae by multiple environmental factors: A dynamic balance hypothesis. New Phytol. **137:** 629–638.

KARALI, E. F., AND C. A. PRICE. 1963. Iron, porphyrins and chlorophyll. Nature **198:** 708.

MARTIN, J. H., AND S. E. FITZWATER. 1988. Iron deficiency limits phytoplankton growth in the Northeast Pacific subarctic. Nature **331:** 341–343.

MILLER, W. L., D. W. KING, J. LIN, AND D. R. KESTER. 1995. Photochemical redox cycling of iron in coastal seawater. Mar. Chem. **50:** 63–77.

MOORE, J. K., S. C. DONEY, D. M. GLOVER, AND I. Y. FUNG. 2002. Iron cycling and nutrient-limitation patterns in surface waters of the World Ocean. Deep-Sea Res. (II Top. Stud. Oceanogr.) **49:** 463–507.

MOREL, F. M. M., R. J. M. HUDSON, AND N. M PRICE. 1991. Limitation of productivity by trace metals in the sea. Limnol. Oceanogr. **36:** 1742–1755.

———, AND N. M. PRICE. 2003. Biogeochemical cycles of trace metal in the oceans. Science **300:** 944–947.

NELSON, D. M., AND L. E. BRAND. 1979. Cell division periodicity in 13 species of marine phytoplankton on a light:dark cycle. J. Phycol. **15:** 67–75.

NIELSEN, M. V. 1992. Irradiance and daylength effects on growth and chemical composition of *Gyrodinium aureolum* Hulburt in culture. J. Plankton Res. **14:** 811–820.

OWENS, T. G., P. G. FALKOWSKI, AND T. E. WHITLEDGE. 1980. Diel periodicity in cellular chlorophyll content in marine diatoms. Mar. Biol. **59:** 71–77.

PFANNSCHMIDT, T. A. 2003. Chloroplast redox signals: How photosynthesis controls its own genes. Trends Plant Sci. **8:** 33–41.

RAVEN, J. A. 1988. The iron and molybdenum use efficiencies of plant growth with different energy, carbon, and nitrogen sources. New Phytol. **109:** 279–287.

———. 1990. Predictions of Mn and Fe use efficiencies of phototrophic growth as a function of light availability for growth and C assimilation pathway. New Phytol. **116:** 1–18.

———, M. C. W. EVANS, AND R. E. KORB. 1999. The role of trace metals in photosynthetic electron transport in O_2-evolving organisms. Photosynth. Res. **60:** 111–149.

RUE, E. L., AND K. W. BRULAND. 1997. The role of organic complexation in ambient iron chemistry in the equatorial Pacific Ocean and the response of a mesoscale iron addition experiment. Limnol. Oceanogr. **42:** 901–910.

SAKSHAUG, E., AND K. ANDERSEN. 1986. Effect of light regime upon growth rate and chemical composition of a clone of *Skeletonema costatum* from the Trondheimsfjord, Norway. J. Plankton Res. **8:** 619–637.

———, ———, AND D. A. KIEFER. 1989. A steady state description of growth and light absorption in the marine plankton diatom *Skeletonema costatum.* Limnol. Oceanogr. **34:** 198–205.

SPILLER, S., AND N. TERRY. 1980. Limiting factors in photosynthesis. II. Iron stress diminishes photochemical capacity by reducing the number of photosynthetic units. Plant Physiol. **65:** 121–125.

SUNDA, W. G. 1988/1989. Trace metal interactions with phytoplankton. Biol. Oceanogr. **6:** 411–442.

———. 2001. Bioavailability and bioaccumulation of iron in the sea, p. 41–84. *In* D. R. Turner and K. A. Hunter [eds.], The biogeochemistry of iron in seawater. Wiley.

———, AND S. A. HUNTSMAN. 1992. Feedback interactions between zinc and phytoplankton in seawater. Limnol. Oceanogr. **37:** 25–40.

———, AND ———. 1995*a*. Cobalt and zinc interreplacement in marine phytoplankton: Biological and geochemical implications. Limnol. Oceanogr. **40:** 1404–1417.

———, AND ———. 1995*b*. Iron uptake and growth limitation in oceanic and coastal phytoplankton. Mar. Chem. **50:** 189–206.

———, and ———. 1997. Interrelated influence of iron, light, and cell size on growth of marine phytoplankton. Nature **390:** 389–392.

———, AND ———. 2003. Effect of pH, light, and temperature on Fe-EDTA chelation and Fe hydrolysis speciation in seawater. Mar. Chem. **84:** 35–47.

TERBORGH, J. W., AND K. V. THEMANN. 1964. Interactions between daylength and light intensity in the growth and chlorophyll content of *Acetabularia crenulata.* Planta **63:** 83–98.

TERRY, N. 1980. Limiting factors in photosynthesis. I. Use of iron stress to control photochemical capacity *in vivo.* Plant Physiol. **65:** 114–120.

VÅRUM, K. M., K. ØSTGAARD, AND J. GRIMSRUD. 1986. Diurnal rhythms in carbohydrate metabolism of the marine diatom *Skeletonema costatum* (Grev.) Cleve. J. Exp. Mar. Biol. Ecol. **102:** 249–256.

VERITY, P. G. 1981. Effects of temperature, irradiance, and daylength on the marine diatom *Leptocylindrus danicus* Cleve. I. Photosynthesis and cellular composition. J. Exp. Mar. Biol. Ecol. **55:** 79–91.

WAITE, T. D., R. SZYMCZAK, Q. I. ESPEY, AND M. J. FURNAS. 1995. Diel variations in iron speciation in northern Australian shelf waters. Mar. Chem. **50:** 79–91.

Received: 30 June 2003
Accepted: 30 March 2004
Amended: 6 April 2004